IEEE Access
Multidisciplinary | Rapid Review | Open Access Journal

Received October 13, 2020, accepted October 19, 2020, date of publication October 23, 2020, date of current version November 5, 2020.

Digital Object Identifier 10.1109/ACCESS.2020.3033314

Compact Wideband Four Element Optically Transparent MIMO Antenna for mm-Wave 5G Applications

ARPAN DESAI[1,2], CONG DANH BUI[1,2], JAY PATEL[3], (Graduate Student Member, IEEE), TRUSHIT UPADHYAYA[4], (Senior Member, IEEE), GANGIL BYUN[5], (Member, IEEE), AND TRUONG KHANG NGUYEN[1,2], (Member, IEEE)

[1]Division of Computational Physics, Institute for Computational Science, Ton Duc Thang University, Ho Chi Minh City 758307, Vietnam
[2]Faculty of Electrical and Electronics Engineering, Ton Duc Thang University, Ho Chi Minh City 758307, Vietnam
[3]New York Institute of Technology, New York, NY 10023, USA
[4]Department of Electronics and Communication Engineering, CHARUSAT, Changa 388421, India
[5]School of Electrical and Computer Engineering, Ulsan National Institute of Science and Technology, Ulsan 44919, South Korea

Corresponding author: Truong Khang Nguyen (nguyentruongkhang@tdtu.edu.vn)

ABSTRACT A four-element compact wide-band optically transparent MIMO antenna with a full ground plane is proposed. The four elements transparent MIMO system has a compact size of 24×20 mm^2 with the undivided ground plane as most of the real-time systems demand a common reference. The complete antenna system achieves around 85% transparency due to a combination of AgHT-8 and Plexiglas which forms the transparent conductive patch/ground and substrate, respectively. The antenna geometry leads dual-band operation ranging from 24.10 - 27.18 GHz (Impedance bandwidth = 12%) and 33 - 44.13 GHz (Impedance bandwidth = 28.86%) targeting the mm-wave 5G applications. The 4-element antenna system achieves isolation between inter-elements > 16 dB and maximum gain value of greater than 3 dBi with more than 75% efficiency. The proposed transparent MIMO antenna is evaluated in terms of diversity gain (DG), envelope correlation coefficient (ECC), total active reflection coefficient (TARC), and mean effective gain (MEG) where decent MIMO performance with isolation more than >16 dB between the adjacent and other elements is achieved. Transparent MIMO antenna achieves directional patterns for the operating band with the value of DG > 9, ECC < 0.1, TARC value less than −15dB, and the ratio of MEG within the agreed limit of ±3 dB confirming acceptable MIMO/diversity performance.

INDEX TERMS Transparent, MIMO, compact, 5G, mm-wave.

I. INTRODUCTION

The emergence of the 5G standard has established an enormous increase in the throughput of data where theoretically the channel capacity will be increased 1,000 times. This increase depends on several supporting technologies in 5G, where the spectrum in the millimeter-wave range can be utilized as the bandwidth is available in an excessive manner. 5G is expected to deliver higher data to a greater number of devices with higher consistency and lower latency than previous technologies. The frequency band working in mm-wave is explored which can accommodate a larger group of subscribers as it offers numerous advantages, such as high resolution, data transfer at high-speed, smaller form factor allowing smaller dimensions of antenna sizes, low interference making systems with higher immunity towards cramming, cost-effectiveness and increased security making the mm-wave band an ideal candidate for 5G technology [1], [2]. Such technology demands upgraded communication systems that can offer better spectral efficiency antennas with restricted power levels.

Multiple-input multiple-output (MIMO) is one of the key technologies to enhance the performance of 5G technology. Systems with MIMO antenna should maintain small inter-element distance, lower correlation values, and high isolation between inter elements [3]. The biggest advantage of using the MIMO network compared to a regular one is lower spectrum utilization since it can increase the wireless

The associate editor coordinating the review of this manuscript and approving it for publication was Kai Lu.

connection capacity. The link reliability and data rate of the system can be improved if the transmitter/receiver has a greater number of antennas as it leads to more signal paths and hence better performance.

The prevailing infrastructure needs to be upgraded to implement an interconnected system amid end users, buildings, and various other transportation services. The installation of 5G networks faces challenges when it comes to the interconnection of open-air systems and alterations between indoor and outdoor communications. Signal degradation is inevitable due to scattering and reflection. To avoid it, network repeaters should be incorporated with existing infrastructure. One of the ways to implement 5G enabled devices is by incorporating transparent antennas which solves the need for 5G wireless networks while maintaining the aesthetics of the surrounding. The transparency of such antennas is due to the thin-film materials which owe low value of electrical resistivity and high transparency [4]–[6]. A large selection of conductive oxide materials is available for such antennas, comprising conductive polymers such as AgHT (a silver-coated polyester film), Indium Tin Oxide (ITO), Zinc Oxide (ZnO), and Fluorine oxide (FTO) [7]. The wide acceptance of Ag is due to its optical loss and low electrical resistivity among other metals over the visible spectral range. The Indium prices along with being a rare earth metal confine its use whereas Zinc and Fluorine doped oxide sheets are still in development stages making AgHT as the best contender for making transparent antennas [8], [9]. Though graphene with outstanding optical transparency is a strong contender for its use at high frequency, manufacturing at the nanoscale needs state of the art fabrication facilities and thus might not be available commercially like AgHT-8 and AgHT-4 [10], [11].

Devices working in the mm-wave band impose the implementation of MIMO antenna systems to fulfill the strict design requirements while achieving gain, bandwidth, footprint, correlation, and isolation. As antenna elements are more in MIMO systems, the smaller antenna element size is favorable to achieve a compact design while achieving the acceptable isolation between elements [12], [13]. Many such 4 element MIMO antennas using various techniques for achieving diversity parameters are proposed. A 4-element antenna system for sub 6 GHz 5G laptop applications is proposed in [14] which uses inverted F-shaped antennas. In [15], MIMO antenna radiating in the Wi-Fi frequency band using a combination of 3 dipoles and 1 slot antenna is proposed. A 4-port compact MIMO antenna for WLAN application is proposed in [16] where only simulated results are presented for diversity performance. A tightly arranged MIMO antenna with lumped components is presented in [17] for 5G mobile stations. A MIMO antenna consisting of a meander dipole and parabolic reflector is proposed in [18] for WLAN applications. A MIMO antenna for satellite applications using defected ground is proposed in [19]. A compact MIMO antenna working in the ISM band is proposed in [20] for biomedical applications. Few more MIMO antennas designed for various 5G [21], WLAN [22], 4G LTE [23], and other wireless applications [22]–[29] are proposed. In [30], an eight-element MIMO antenna applicable for mobile terminals working in sub 6GHz 5G band working from 3.3 - 3.6 GHz is proposed. In [31], a UWB MIMO antenna working in the frequency range of 3.1–10.6 GHz is proposed. A box folded MIMO antenna for LTE handsets is proposed in [32] which resonates from 1.8 -2.8 GHz. A compact 4 element antenna working in the frequency band of 2 GHz to 10.6 GHz is proposed for wireless applications [33]. A compact four-port orthogonally polarized slotted MIMO antenna is proposed in [34] for WiMAX application. A 3D printed 4 $\times$ 3 MIMO antenna working in the frequency band of 26 GHz- 29.8 GHz (13.62%) is proposed in [35]. A dual-element planar MIMO antenna resonating in 26 GHz-35 GHz (29.5%), 36 GHz - 42 GHz (15.38%) is proposed in [36] for 5G applications. One more dual-element MIMO antenna is reported in [37] for 5G communications which is resonating in 26.65 GHz-29.2 GHz (9.1%) and 36.95GHz-39.05 GHz (5.52%) bands.

Some of the selected MIMO antennas are compared in terms of operating frequency, the material used, radiation efficiency, and diversity parameters as shown in Table 1. The MIMO antennas in the literature were mainly proposed for frequency band between 1-10 GHz [14], [24], [28] with very less work carried out in the mm-wave band [35]–[37]. More importantly, the transparent antennas are still not tested to work for mm-wave MIMO applications [4]–[6].

In this article, a transparent four-element MIMO antenna is presented, where square ring-shaped antennas are arranged in a common ground plane. The structure achieves the resonance at a lower frequency in addition to a wideband resonance at the higher side in the mm-wave frequency band. The proposed optically transparent MIMO antenna is capable of functioning in the 24.10 - 27.18 GHz and 33 - 44.13 GHz frequencies for 5G applications. The transparent four-element MIMO system has acceptable inter-element isolation, compact footprint with the low value of total active reflection coefficient (TARC) and envelope correlation coefficient which are validated by simulations carried out in Finite Element Method (FEM) based Ansys High-Frequency Structure Simulator (HFSS), fabricating prototypes and measuring the experimental results. The comparison of transparent 4 element MIMO antenna is carried out with other MIMO antennas from literature as listed in table 1 where it can be observed that the proposed transparent MIMO antenna outperforms other MIMO antenna from literature based on optical transparency, smallest size, no extra isolation element, full ground plane, resonating in the mm-wave frequency band and satisfactory diversity parameters which makes the antenna suitable for smart devices using 5G mm-wave spectrum.

II. ELEMENTARY ANTENNA GEOMETRY

The single element transparent structure of the antenna fed by a microstrip line optimized at 50 Ω with a full ground plane is depicted in Fig. 1 is tested before implementing a 4 elements transparent MIMO antenna.

TABLE 1. Comparison of proposed transparent MIMO antenna with other MIMO antennas from literature.

Reference	Physical Dimension (mm) Element Number	Substrate	Radiation efficiency (%)	MIMO Parameters			Operating frequency
				Isolation (dB)	ECC	Diversity Gain	
4	105*105 2elements	Plexiglas (Transparent)	~74	>12	<.002	9.95-9.99	2.23 GHz-2.46 GHz (9.8%) 3.22 GHz-4.04 GHz (22.58%)
5	40*40 2 elements	Glass (Transparent)	43 46	--	--	--	2.4 GHz-2.48 GHz (3.27%) 5.15GHz-5.8 GHz (11.87%)
6	150*70 2 elements	Glass (Transparent)	--	--	--	--	4.5 GHz – 5.3 GHz (16.32%)
14	3*64*1.4 4 elements	FR-4	≥35	≥10	<0.3	--	3.3 GHz-3.6 GHz (8.69%) 4.8 GHz-5 GHz (4.08%)
24	50*50*1.6 4 elements	FR-4	NA	NA	<0.15 (uniform) < 0.45 (indoor) < 0.45 (outdoor)	--	2 GHz-4.91GHz (84.22%) 6.41 GHz - 12 GHz (60.72%)
28	46*20*1.6 4 elements	FR-4	60 (port 1,2) 85 (port 3,4)	12	0.01 (2.45 GHz) 0.27 ~ 0.11 (5.5 GHz)	--	2.4 GHz-2.5 GHz (4.08%) 4.9 GHz-5.8 GHz (16.82%)
35	52.9*57*3 4 elements	3D printing and JMT process	--	>28	--	>9.97	26 GHz- 29.8 GHz (13.62%)
36	26*11 2 elements	Rogers 4003C	99.5 98.6	>25	<0.001	10	26 GHz - 35 GHz (29.5%) 36 GHz - 42 GHz (15.38%)
37	26*14 2 elements	Rogers RT/Duroid 5880	--	>20	<0.001	10	26.65 GHz-29.2 GHz (9.1%) 36.95GHz-39.05 GHz (5.52%)
Proposed Antenna	**24*20*1.85 4 elements**	**Plexiglass (Transparent)**	**75**	**>16dB**	**<0.1**	**>9.5**	**24.10 - 27.18 GHz (12.01%) 33 - 44.13 GHz (28.86%)**

The antenna is comprised of AgHT-8 (Silver sandwiched between tin oxide layers) which forms a conductive patch and full ground plane with Plexiglas as the substrate. The single element transparent structure has an overall dimension of 12 mm × 10 mm with a total thickness of 1.85 mm. The Plexiglas substrate has permittivity (εr), loss tangent (Tan δ), and thickness value of 2.3, 0.0003, and 1.48 mm, respectively. AgHT-8 has the conductivity and thickness of 125,000 S/meter, and 0.177mm, respectively. ANSYS HFSS software is used for simulating the proposed antenna.

The undivided ground plane is used as a common reference which is suitable for most of the real-time systems.

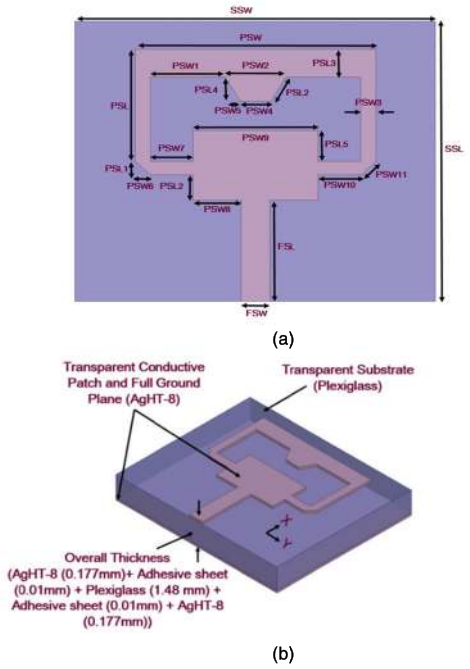

FIGURE 1. Single Element Transparent Antenna Geometry (a) Top View (b) Perspective View.

The optimized parameters of a single element transparent antenna are illustrated in Table 2.

TABLE 2. Single element antenna geometry parameters.

Parameters	Dimension (mm)	Parameters	Dimension (mm)
SSW	12	PSW1	2.5
SSL	10	PSW2	2
PSW	8	PSW3	0.5
PSL	4	PSW4	1
PSL1	0.5	PSW5	0.5
PSL2	0.9	PSW6	0.5
PSL3	1	PSW7	1.416
PSL4	0.866	PSW8	1.609
PSL5	1.1	PSW9	4.168
PSW10	1.416	PSW11	0.707
FSL	3.6	FSW	0.98

The top and the front view of the fabricated prototype of a single element transparent antenna is as shown in Fig. 2 where the background is visible due to the optical transparency of the antenna structure. The proposed antenna is optically transparent and is fabricated using a conductive oxide sheet which is patterned using a laser cutter. The sheet is attached to the transparent Plexiglas substrate after patterning using extra thin double-sided adhesive tape. The SMA connector is interfaced using conductive silver epoxy to evade the hot soldering process. The complex antenna geometry leads to fabrication imperfections since the proposed antenna is very small in size and as a result, the patch is designed in such a manner to achieve the least complexity in fabrication. In addition, the proposed antenna element allows for a compact

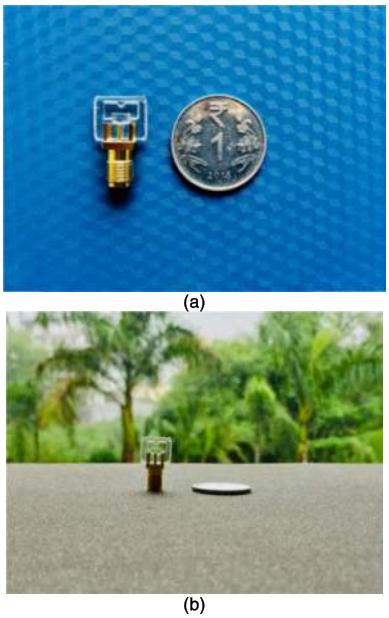

FIGURE 2. Fabricated Single Element Transparent Antenna (a) Top View (b) Front View.

MIMO configuration with close distance while still meeting the criteria for achieving the required isolation at mm-wave frequencies [17].

III. PARAMETRIC ANALYSIS

The design steps of the antenna in terms of simulated reflection coefficient are shown in Fig. 4 where the stepwise analysis of antenna performance improvement from the initial stage to the final proposed antenna in terms of achieving the dual-frequency band operation working in the mm-wave band for 5G applications has been carried out. The reasonable bandwidth performance is visible in Ant#1 however the targeted frequency bands are not achieved.

The rectangular patch supports different resonant modes which are a function of its dimensions and each of these modes has a distinct impedance. The microstrip edge coupled ANT#1 has been designed to provide an impedance match over a small frequency range resulting in the excitation of a higher-order mode in addition to the fundamental mode. The two distinct modes can be recognized from the surface current distribution as shown in Fig. 3.

Ant#2 depicts improvement in bandwidth at the lower band however it is still not achieving the frequency band useful for 5G applications on the lower side. The mm-wave frequency matching is still not achieved after the second step so the two arms pointing upwards are added in ANT#3 which improved the results at lower and higher bands however the bandwidth at the higher side deteriorates. Further modification in terms of closing the patch, cutting the side edges on the bottom side of the conductive patch, and the addition of conductive container shaped structure on the upper side leads to performance improvement as shown for ANT#4. The desired frequency band ranging from 24.10 - 27.18 GHz and 33 - 44.13 GHz

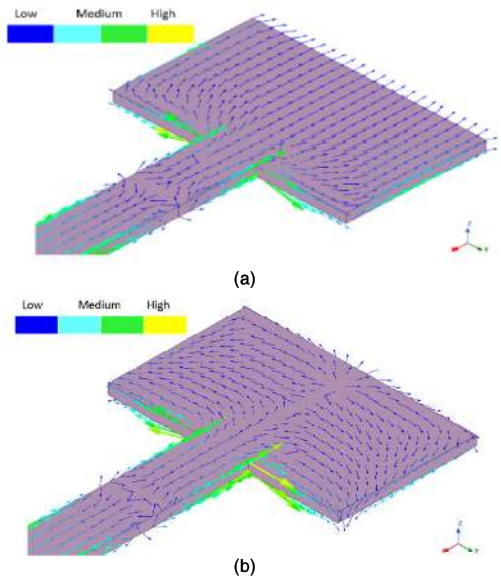

FIGURE 3. Current Distribution of ANT#1 at (a) 25.52 GHz (b)35.20 GHz.

is achieved in the final proposed design with a reflection coefficient value greater than 20 dB for targeted bands.

The width variation of container shaped structure ''PSW4'' near the upper side of the patch helps in optimizing the frequency and achieving an acceptable level of reflection coefficient at the lower side providing the desired band for 5G applications as shown in Fig. 5 (a).

Simulated S11 of the proposed single element transparent antenna for different thickness of patch arm ''PSW3'' is illustrated in Fig. 5 (b). It is established that the width of container shaped structure (PSW4) = 0.5 mm and arm width (PSW3) = 0.5 mm provides the impedance bandwidth ranging from 24.10-27.18 GHz and 33 - 44.13 GHz with reflection coefficient greater than 20 dB at bands of interest.

It can be observed in Fig. 6 that the reflection coefficient varies a lot due to the variation of ground plane length. Ground length (gl) = 7 mm also gives good results however the frequency band on the higher side is not covering the mm-wave band applicable for 5G. The desired frequency band in a single element transparent antenna is achieved for ground length (gl) = 10 mm which covers the full ground plane as illustrated in Fig. 6.

Fig. 7 illustrates the surface current distribution of a single element transparent antenna at three frequencies. It can be observed that at 25.56 GHz, the current is distributed evenly across the patch while at higher frequency bands of 35.47 GHz and 40 GHz, the current traverses along the feed-line and sides of the conductive patch. Very less current is observed at the top side of the patch which can help in reducing the coupling between elements placed opposite to the antenna.

IV. 4-ELEMENT TRANSPARENT MIMO ANTENNA CONFIGURATION

A four-element transparent MIMO antenna is realized after carrying out the analysis of a single element transparent antenna as depicted in Fig. 8.

The symmetrically placed antenna is arranged in an upper-lower manner is designed on the Plexiglas substrate having a size of $24 \times 20 \times 1.85$ mm^3 with a complete ground plane. The horizontal and vertical separation between the antenna elements is 4 mm and 2 mm, respectively which is chosen after carrying out the isolation analysis by varying the distance between horizontal and vertical elements as shown in Fig. 9 (a,b).

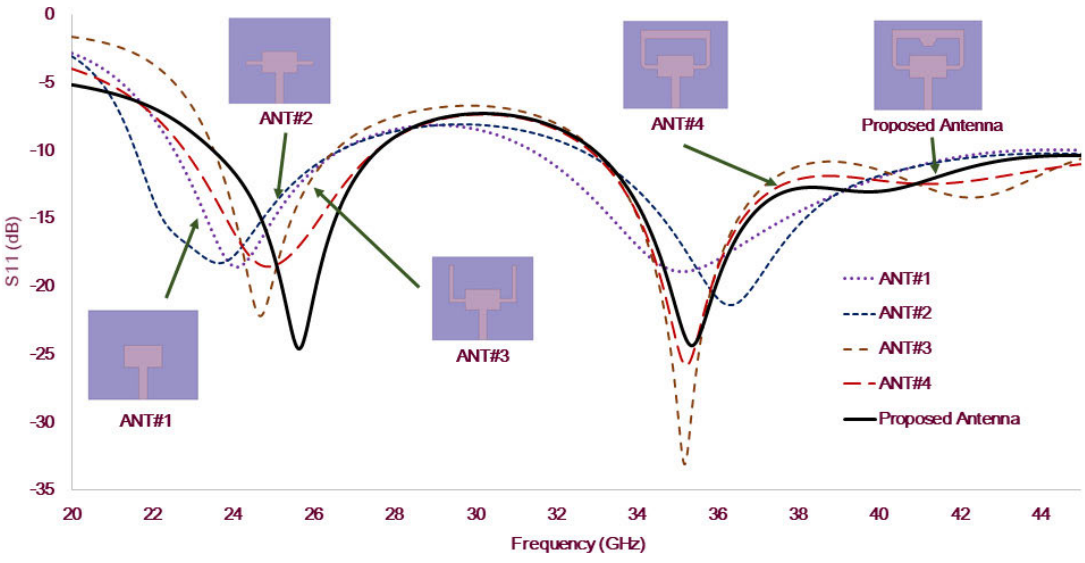

FIGURE 4. S11 of the antenna evolution.

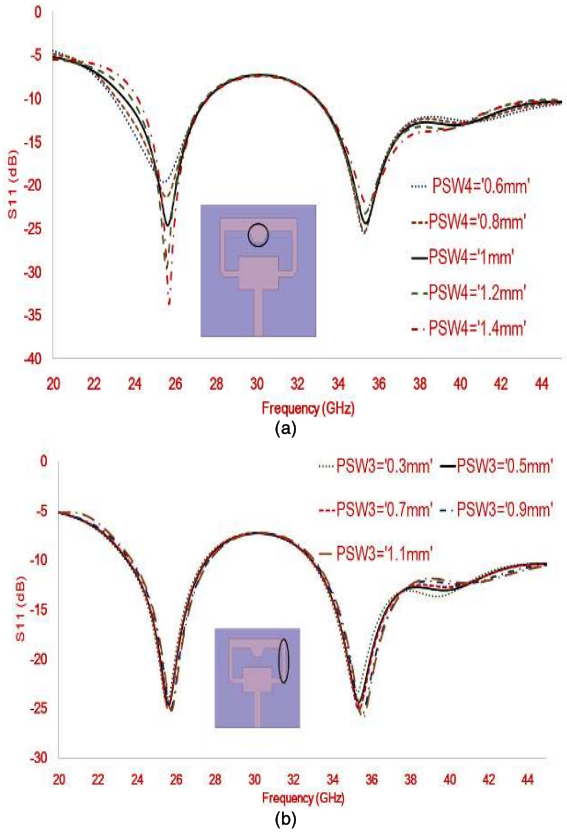

FIGURE 5. Effect on S11 due to variation of (a) Psw4 (b) Psw3.

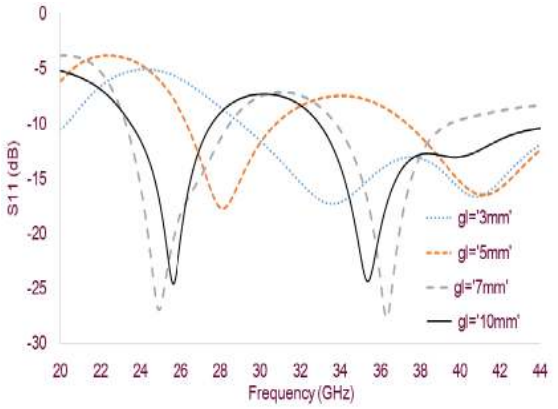

FIGURE 6. Effect on S11 due to variation of the ground plane in single element configuration.

The single element antenna is replicated along a horizontal direction where the condition of the distance between two elements is maintained at $\lambda/3$. Two other cases where the distance between two elements $= \lambda/2$ and $\lambda/4$ are also discussed to understand the effect of mutual coupling as shown in Fig. 9 (a). The antenna shows the best isolation at $\lambda/2$ for the proposed band whereas lower isolation is observed for $\lambda/4$ distance. The tolerances distance of $\lambda/3$ is chosen since it shows the isolation at an acceptable level as mentioned in [17] while maintaining the compact purpose. The distance along the vertical direction, seen from Fig. 9 (b), is varied

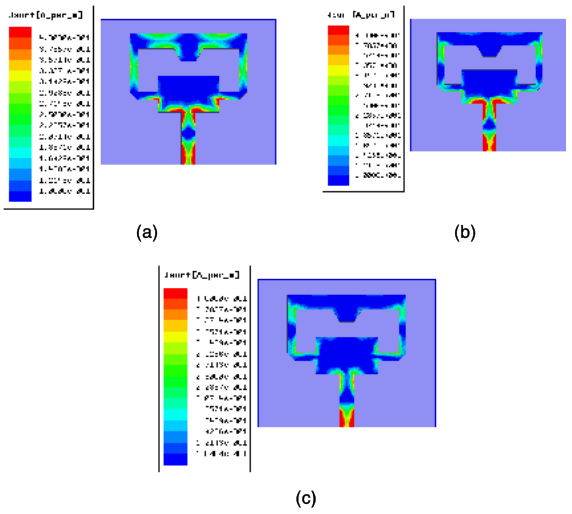

FIGURE 7. Current distribution of single element transparent antenna at (a) 25.56 GHz (b) 35.47 GHz (c) 40 GHz.

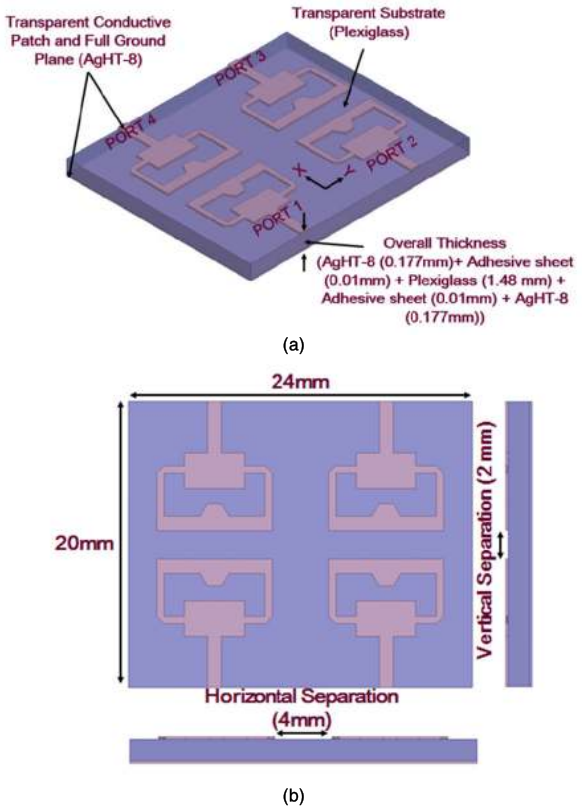

FIGURE 8. Four Element Transparent MIMO Antenna Geometry (a) Perspective View (b) Top View.

from 1 mm to 3 mm where it shows that increase the distance between elements leads to higher isolation. The vertical distance between two elements is chosen as 2 mm where an isolation level of 19 dB is achieved while maintaining the symmetry of the design.

The fabricated prototype of 4 elements transparent MIMO antenna is depicted in Fig. 10 where the transparency of the antenna is clearly visible.

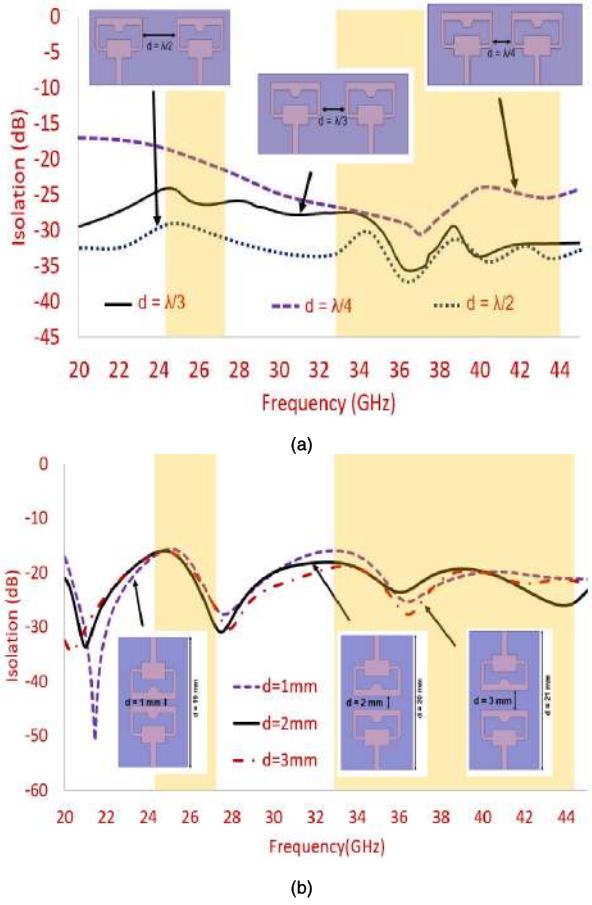

FIGURE 9. Isolation levels of 2 element MIMO antenna (a) Horizontal direction (b) Vertical direction.

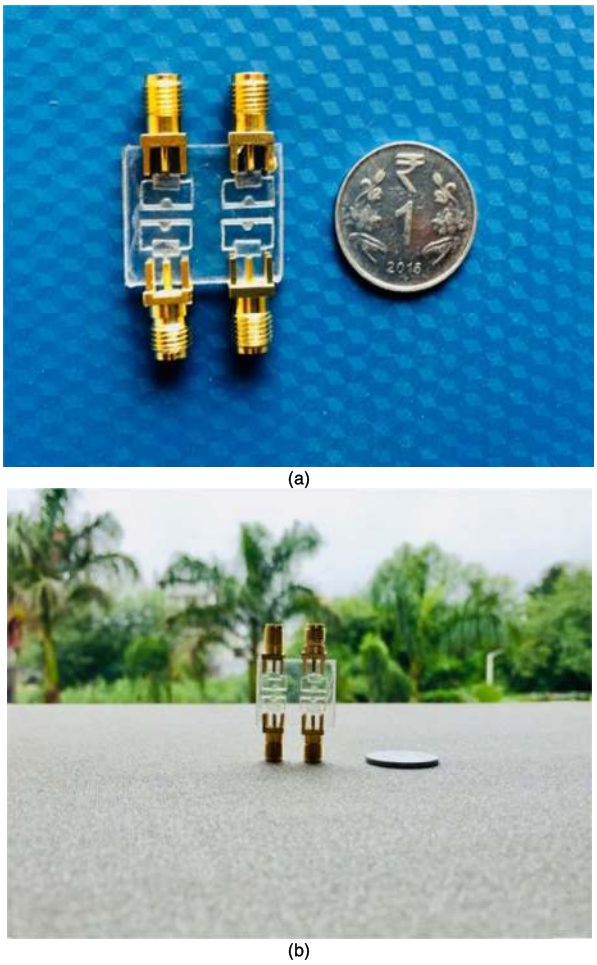

FIGURE 10. Fabricated 4 element MIMO antenna (a) Top View (b) Front View.

V. RESULTS AND DISCUSSION

The reflection coefficient of a single element transparent prototype is measured using the Keysight N9962A vector network analyzer as shown in Fig. 11. The measured reflection coefficient (S11) is better than 10 dB for the frequency band of 23.51 – 26.54 GHz and 33.11 – 44.02 GHz which matches well with the simulated results. The shift at the lower side of the frequency band is due to connector interfacing, and fabrication tolerances. The frequency bands achieved after simulation and measured results are within the limits proposed by various countries for 5G. Table 3 depicts the 5G applications of the proposed transparent 4 element MIMO antenna for the targeted frequency bands. The promising applications, such as communication between Machine to Machine (M2M) and the Internet of Things (IoT) for smart cities, need to be investigated by the industry for 5G bands to achieve the multitude of applications.

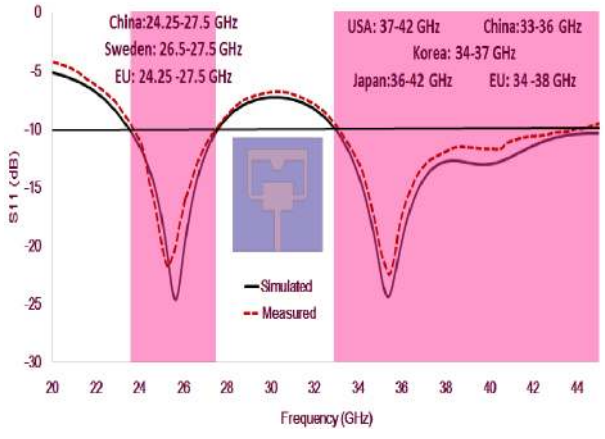

FIGURE 11. Simulated (Solid) and Measured (Dashed) S11 of Single Element Transparent Antenna.

VI. MIMO DIVERSITY ANALYSIS

Diversity analysis is a must when proposing a MIMO antenna along with other fundamental parameters. The diversity parameters include mutual and isolation coupling, correlation coefficient (ECC), diversity gain (DG), total active reflection coefficient (TARC), and (Mean effective gain) MEG. In applications using MIMO antennas, multiple antennas transmit the signals and as a result, it is expected that those are uncorrelated and independent. In reality, the mutual coupling arises due to the generation of voltage in adjacent antenna elements due to the induction of current in another antenna [12].

TABLE 3. Proposed MIMO antenna target frequency band covering various applications for different countries *.

Countries	Target Frequency Band Range (GHz)	Applications	Target Frequency Band Range (GHz)	Applications
Europe	24.25-27.5	-Improved residential connections -Homes and businesses using fixed wireless access -Regular and autonomous trains, buses, and cars -Smart Healthcare	34-38	-IoT applications in Smart cities -5G WiFi routers and repeaters
China	24.25-27.5		33-36	
Japan	--		36-42	
Korea	--		34-37	
USA	--		37-42	
Sweden	26.5-27.5		37.20-38	

**https://www.cablefree.net/wirelesstechnology/4glte/5g-frequency-bands-lte/*

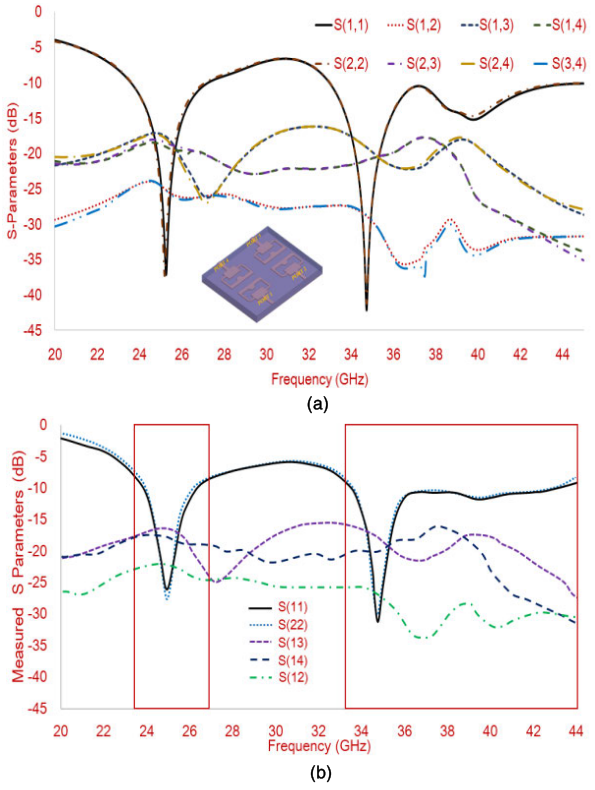

FIGURE 12. S-Parameters results of proposed 4 elements transparent MIMO antenna (a) Simulated (b) Measured.

Fig. 12 displays the simulated and measured S-parameters of the Transparent MIMO antenna. It is observed that the MIMO system achieves simulated impedance bandwidth of 12% (24.10 - 27.18 GHz) and 28.86% (33 - 44.13 GHz) with measured impedance bandwidth of 9.63% (23.91 – 26.22 GHz) and 25.07% (33.62 - 43.26 GHz) for S11 and S22.

Coupling between diagonal elements (1,3 and 2,4) is well below −16dB with a considerable decrease in the mutual coupling at higher frequency bands. The adjacent elements (1,2 and 3,4) exhibits coupling value below −24dB as compared to the elements placed in the vertical direction having mutual coupling value below −19dB. The inter-element distance attributes to the coupling in the vertical direction as compared to the horizontal direction as vertically the elements are separated by 2mm while horizontally, the elements have a separation of 4mm. Thus, it can be observed from Fig. 12 (a) and (b) that satisfactory performance is achieved for isolation between inter-elements in simulated and measured results for Transparent MIMO antenna without using any complex isolation geometry. To ensure maximum antenna energy radiation, negligible energy in MIMO systems should be lost in the other antenna ports which are terminated by the matched load which means that |Sij| needs to be suppressed to a very low value.

The 3D radiation pattern of 4 elements transparent MIMO antenna is depicted in Fig. 13 by giving excitation at port 1 and keeping other ports terminated to matched loads. The gain values at 25.25 GHz, 34.74 GHz, and 39.80 GHz are 3.84 dBi, 4.56 dBi, and 2.91 dBi, respectively. The 3D radiation pattern shows a directional pattern at three frequency bands (25.25 GHz, 34.74 GHz, and 39.80 GHz) where the maximum gain is observed in the direction away from the antenna elements thus avoiding the mutual coupling and making it suitable for MIMO operation.

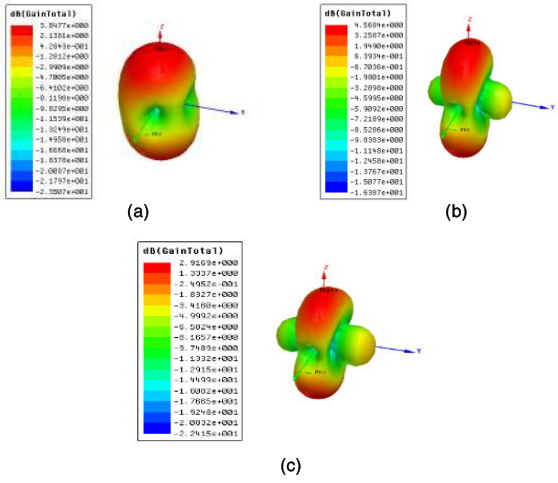

FIGURE 13. 3D Polar plot of 4 element MIMO antenna with port 1 excited keeping other ports terminated at matched load at (a)25.25 GHz (b)34.74 GHz (c)39.80GHz.

Fig. 14 shows the simulated and measured 2D radiation patterns for the fabricated transparent MIMO prototype. The patterns along the XY-plane (E Plane) and YZ-plane (H Plane) for element-1 are measured in an anechoic chamber by terminating the additional antenna ports with matched loads for targeted frequency bands. The co/cross-polarization of transparent MIMO antenna shows separation greater

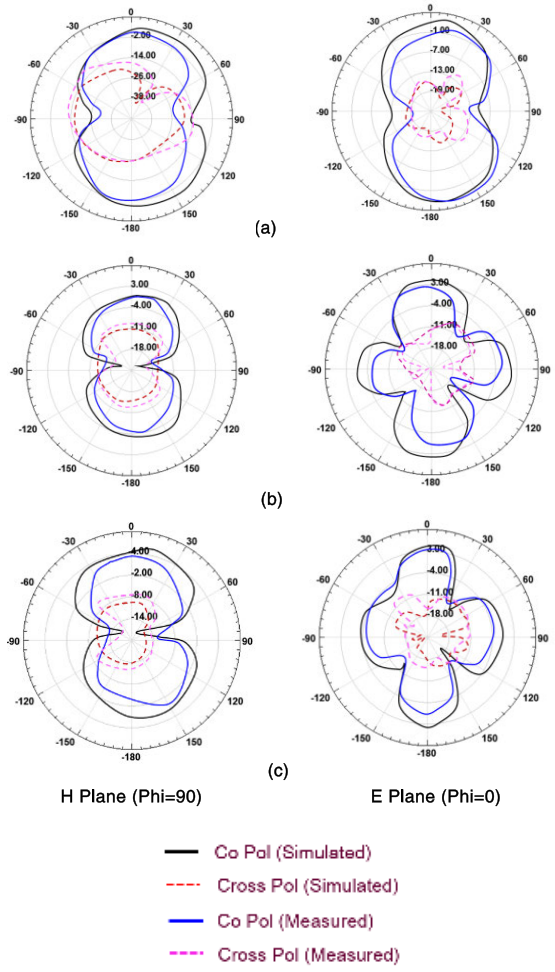

FIGURE 14. Simulated and measured Co/Cross Pol pattern of the proposed 4 element MIMO in E plane and H plane: (a) 25.25 GHz (b) 34.74 GHz, (c) 39.80 GHz.

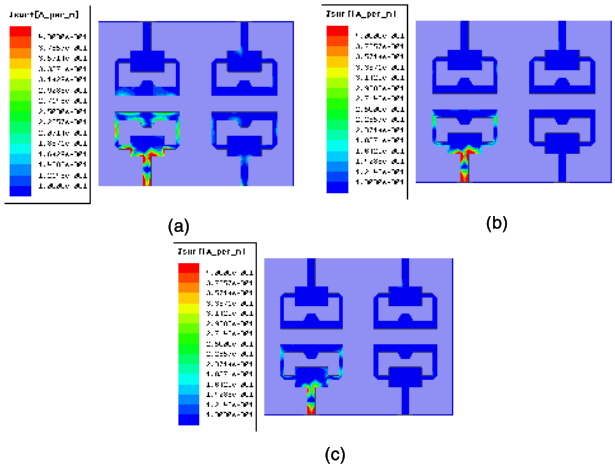

FIGURE 15. Current distribution of 4 element MIMO by exciting port 1 and keeping other ports terminated to matched loads at (a) 25.25 GHz (b) 34.74 GHz (c) 39.80 GHz.

than −15dB where good agreement occurs between measured and simulated radiation patterns.

To further examine the coupling between antenna elements, the surface currents at three frequencies (25.25 GHz, 34.74 GHz, and 39.80 GHz) are as shown in Fig. 15 by exciting port 1 and keeping other ports terminated to matched loads. The surface currents are confined to the antenna excited by port 1 and very less current distribution is observed at the other possible three locations. The current distribution at lower frequency shows less confinement as the adjacent elements show some amount of surface currents linked to it.

The diversity of a system is greatly dependent on the correlation coefficient and it acts as an important parameter for the systems providing diversity. The signals received can have a great correlation in the diversity systems. The similarity degree between the received signals can be measured by the correlation coefficient which is a statistical and mathematical tool whose modulus value ranges from 0 to 1. The ECC is calculated with the help of a 3D radiation pattern as recommended in [12] by referring to (1).

$$\rho_e = \frac{\left| \iint_{4\pi} [s_i(\vartheta, \varphi) * s_i(\vartheta, \varphi) \, d\Omega] \right|^2}{\iint_{4\pi} |s_i(\vartheta, \varphi)|^2 d\Omega \iint_{4\pi} |s_i(\vartheta, \varphi)|^2 d\Omega} \quad (1)$$

where, Si(θ, Φ) indicates a 3D radiation pattern of the transparent MIMO antenna by exciting ith port, and Ω indicates the solid angle. The Hermitian operator in the form of a product is indicated by an asterisk. The equation requires a 3D polar plot and integral for finding out ECC. The environment for outdoor propagation is considered as uniform. Fig. 16 shows that the proposed transparent MIMO antenna meets the criteria of $\rho e < 0.1$ for the simulated and measured values.

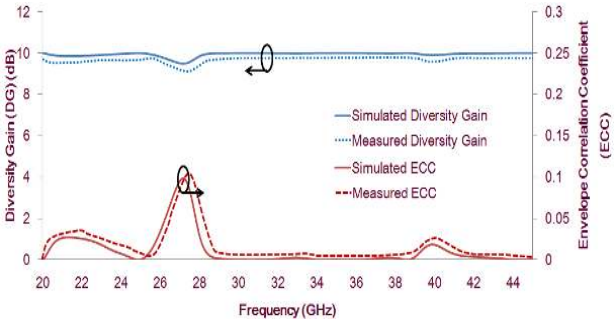

FIGURE 16. Envelope Correlation Coefficient of proposed Transparent MIMO antenna.

In MIMO systems, diversity is attained when various transmitted signals are received by the transmitter through various multiple channel paths due to the presence of more than one antenna in a system. A high value of the signal to noise ratio is achieved if the signals received at the transmitter are uncorrelated and that leads to better reception of the signal. Mathematically, the diversity gain is calculated by referring to (2) [12], [40] which indicates that high diversity gain is

achieved if the correlation coefficient is less. The simulated and measured values of DG are greater than 9.5 dB as shown in Figure 16.

$$DiversityGain(DG) = 10\sqrt[10]{1-(ECC)^2} \tag{2}$$

Characterization of bandwidth and efficiency of the MIMO system is not enough by the scattering matrix [40]. The parameter which characterizes bandwidth and efficiency of the MIMO system accurately is the total active reflection coefficient (TARC). The TARC of the MIMO system can be calculated by using the S parameters. The TARC for a 4-element MIMO antenna is calculated using the equation given in [12], where Sij are the reflection coefficients between various ports of the transparent MIMO antenna. TARC curves with diverse phase combinations are presented in Fig. 17. The TARC value is well below −15 dB which meets the criteria for MIMO performance.

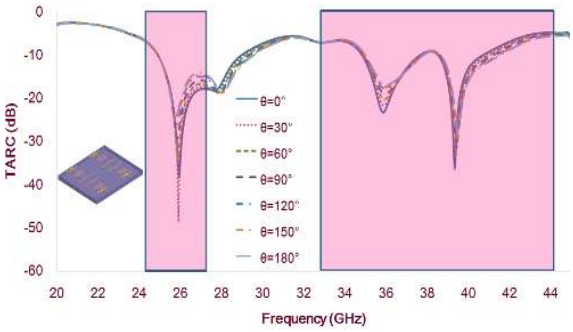

FIGURE 17. Total active reflection coefficient (TARC) of 4 element MIMO antenna.

Mean effective gain is used for quantifying the average strength of signals for each antenna element. It can be calculated by taking the ratio of the mean of received power to incident power. The MEG of the proposed transparent MIMO antenna can be calculated by referring to (3) [40].

$$MEG_i = 0.5\eta_{i,rad} = 0.5[1 - \sum_{j=1}^{N} |S_{ij}|^2] \tag{3}$$

where the value of i ranges from 1 to 4 and Sij indicates the reflection coefficient of antenna elements. The mean effective gain ratio for antenna pair (i,j) given by MEGi/MEGj (in dB) is estimated over the frequency range from 20 – 45 GHz as shown in Fig. 18 where the environment for outdoor propagation is considered as uniform. Average MEG of 1.1 dB is attained for four elements MIMO system where the MEG ratio is confined within the recommended limit of ±3 dB [12].

The simulated and measured value of peak gain and efficiency for the proposed transparent 4 element MIMO antenna is shown in Fig. 19. The MIMO antenna shows reasonable efficiency and gain values for the targeted frequency band with values more than 3 dBi and 75%, respectively thus achieving an efficient system. It is noted that the radiation efficiency of transparent antennas using AgHT-8 is lower

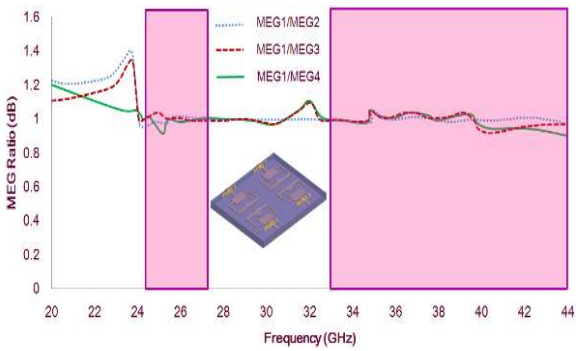

FIGURE 18. MEG Ratio for 4 elements Transparent MIMO antenna.

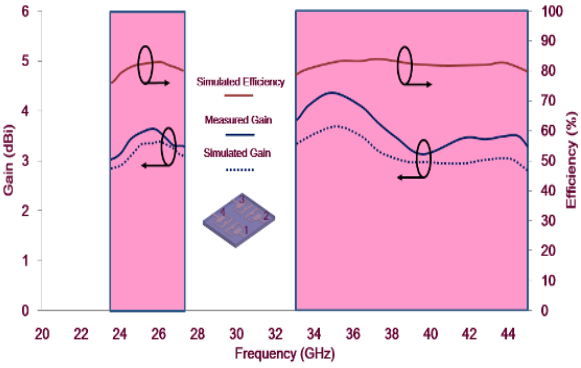

FIGURE 19. Simulated and measured results of Gain and Efficiency for 4 element MIMO antenna.

than that of the metal-based antennas due to the reduced conductivity of AgHT-8 (silver tin oxide sheet) in comparison with the copper.

VII. CONCLUSION

A compact transparent 4 element MIMO antenna with a full ground plane designed using transparent conductive sheet AgHT-8 and Plexiglas with microstrip feed line is proposed. The transparent MIMO system attains 85% optical transparency with impedance bandwidth of 12% and 28.86% at targeted frequency bands along with gain and efficiency values in the range of 3 dBi and 75%, respectively. The diversity parameters including MEG ratio, TARC, ECC, and MEG for 4 elements MIMO with the undivided ground, are within the prescribed limits as suggested in [12] making the proposed configuration potential for its use in low profile smart devices for mm-wave 5G networks.

REFERENCES

[1] A. Desai, T. Upadhyaya, and R. Patel, "Compact wideband transparent antenna for 5G communication systems," *Microw. Opt. Technol. Lett.*, vol. 61, no. 3, pp. 781–786, Mar. 2019.

[2] A. Desai, T. Upadhyaya, J. Patel, R. Patel, and M. Palandoken, "Flexible CPW fed transparent antenna for WLAN and sub-6 GHz 5G applications," *Microw. Opt. Technol. Lett.*, vol. 62, no. 5, pp. 2090–2103, May 2020.

[3] Q. L. Li, S. W. Cheung, D. Wu, and T. I. Yuk, "Optically transparent dual-band MIMO antenna using micro-metal mesh conductive film for WLAN system," *IEEE Antennas Wireless Propag. Lett.*, vol. 16, pp. 920–923, Sep. 2017.

[4] A. Desai, T. Upadhyaya, M. Palandoken, and C. Gocen, "Dual band transparent antenna for wireless MIMO system applications," *Microw. Opt. Technol. Lett.*, vol. 61, no. 7, pp. 1845–1856, Jul. 2019.
[5] Q. L. Li, S. W. Cheung, D. Wu, and T. I. Yuk, "Optically transparent dual-band MIMO antenna using micro-metal mesh conductive film for WLAN system," *IEEE Antennas Wireless Propag. Lett.*, vol. 16, pp. 920–923, Sep. 2017.
[6] K. K. So, B. J. Chen, C. H. Chan, and K. M. Luk, "Study of MIMO antenna made of transparent conductive ITO films," in *Proc. IEEE Asia–Pacific Microw. Conf. (APMC)*, Singapore, Dec. 2019, pp. 515–517.
[7] R. B. Green, M. Toporkov, M. D. B. Ullah, V. Avrutin, U. Ozgur, H. Morkoc, and E. Topsakal, "An alternative material for transparent antennas for commercial and medical applications," *Microw. Opt. Technol. Lett.*, vol. 59, no. 4, pp. 773–777, Apr. 2017.
[8] A. Katsounaros, Y. Hao, N. Collings, and W. A. Crossland, "Optically transparent ultra-wideband antenna," *Electron. Lett.*, vol. 45, no. 14, pp. 722–723, Jul. 2009.
[9] E. Hock, K. W. Leung, X. Fang, and Y. Pan, "Transparent antennas," in *Proc. Wiley Encyclopedia Electr. Electron. Eng.*, 1999, pp. 1–23.
[10] Y. Lee and J.-H. Ahn, "Graphene-based transparent conductive films," *Nano*, vol. 8, no. 3, Jun. 2013, Art. no. 1330001.
[11] M. Bozzi, L. Pierantoni, and S. Bellucci, "Applications of graphene at microwave frequencies," *Radioengineering*, vol. 24, no. 3, pp. 661–669, Sep. 2015.
[12] M. S. Sharawi, "Current misuses and future prospects for printed multiple-input, multiple-output antenna systems [wireless corner]," *IEEE Antennas Propag. Mag.*, vol. 59, no. 2, pp. 162–170, Apr. 2017.
[13] M. S. Sharawi, "Printed multi-band MIMO antenna systems and their performance metrics [wireless corner]," *IEEE Antennas Propag. Mag.*, vol. 55, no. 5, pp. 218–232, Oct. 2013.
[14] S.-C. Chen, C.-W. Chiang, and C.-I. G. Hsu, "Compact four-element MIMO antenna system for 5G laptops," *IEEE Access*, vol. 7, pp. 186056–186064, Dec. 2019.
[15] Y. Cheng, H. Liu, B. Q. Sheng, and L. Zhu, "A compact 4-element MIMO antenna for terminal devices," *Microw. Opt. Technol. Lett.*, vol. 62, no. 9, pp. 2930–2937, Apr. 2020.
[16] C.-Y. Chiu and R. D. Murch, "Compact four-port antenna suitable for portable MIMO devices," *IEEE Antennas Wireless Propag. Lett.*, vol. 7, pp. 142–144, Feb. 2008.
[17] C. Deng, D. Liu, and X. Lv, "Tightly arranged four-element MIMO antennas for 5G mobile terminals," *IEEE Trans. Antennas Propag.*, vol. 67, no. 10, pp. 6353–6361, Oct. 2019.
[18] K. Ding, C. Gao, D. Qu, and Q. Yin, "Compact broadband MIMO antenna with parasitic strip," *IEEE Antennas Wireless Propag. Lett.*, vol. 16, pp. 2349–2353, Jun. 2017.
[19] A. Dkiouak, A. Zakriti, M. El Ouahabi, N. Amar Touhami, and A. Mchbal, "Design of a four-element mimo antenna with low mutual coupling in a small size for satelitte applications," *Prog. Electromagn. Res. M*, vol. 85, pp. 95–104, Sep. 2019.
[20] Y. Fan, J. Huang, T. Chang, and X. Liu, "A miniaturized four-element MIMO antenna with EBG for implantable medical devices," *IEEE J. Electromagn., RF Microw. Med. Biol.*, vol. 2, no. 4, pp. 226–233, Dec. 2018.
[21] H. Huang, X. Li, and Y. Liu, "5G MIMO antenna based on vector synthetic mechanism," *IEEE Antennas Wireless Propag. Lett.*, vol. 17, no. 6, pp. 1052–1055, Jun. 2018.
[22] H. Li, J. Xiong, and S. He, "A compact planar MIMO antenna system of four elements with similar radiation characteristics and isolation structure," *IEEE Antennas Wireless Propag. Lett.*, vol. 8, pp. 1107–1110, Oct. 2009.
[23] M. Ikram, R. Hussain, A. Ghalib, and M. S. Sharawi, "Compact 4-element MIMO antenna with isolation enhancement for 4G LTE terminals," in *Proc. IEEE Int. Symp. Antennas Propag. (APSURSI)*, Jun. 2016, pp. 535–536.
[24] M. S. Khan, A. Iftikhar, R. M. Shubair, A. D. Capobianco, B. D. Braaten, and D. E. Anagnostou, "A four element, planar, compact UWB MIMO antenna with WLAN band rejection capabilities," *Microw. Opt. Technol. Lett.*, vol. 62, no. 10, pp. 3124–3131, May 2020.
[25] S. Pandit, A. Mohan, and P. Ray, "A compact four-element MIMO antenna for WLAN applications," *Microw. Opt. Technol. Lett.*, vol. 60, no. 2, pp. 289–295, Feb. 2018.
[26] R. Anitha, P. V. Vinesh, K. C. Prakash, P. Mohanan, and K. Vasudevan, "A compact quad element slotted ground wideband antenna for MIMO applications," *IEEE Trans. Antennas Propag.*, vol. 64, no. 10, pp. 4550–4553, Oct. 2016.
[27] D. Sarkar and K. V. Srivastava, "A compact four-element MIMO/diversity antenna with enhanced bandwidth," *IEEE Antennas Wireless Propag. Lett.*, vol. 16, pp. 2469–2472, Jul. 2017.
[28] S. Soltani, P. Lotfi, and R. D. Murch, "A dual-band multiport MIMO slot antenna for WLAN applications," *IEEE Antennas Wireless Propag. Lett.*, vol. 16, pp. 529–532, Jul. 2017.
[29] M. Sonkki, D. Pfeil, V. Hovinen, and K. R. Dandekar, "Wideband planar four-element linear antenna array," *IEEE Antennas Wireless Propag. Lett.*, vol. 13, pp. 1663–1666, Aug. 2014.
[30] Z. Xu and C. Deng, "High-isolated MIMO antenna design based on pattern diversity for 5G mobile terminals," *IEEE Antennas Wireless Propag. Lett.*, vol. 19, no. 3, pp. 467–471, Mar. 2020.
[31] L. Yang, M. Xu, and C. Li, "Four-element MIMO antenna system for UWB applications," *Radioengineering*, vol. 28, no. 1, p. 61, Apr. 2019.
[32] L. Yang and T. Li, "Box-folded four-element MIMO antenna system for LTE handsets," *Electron. Lett.*, vol. 51, no. 6, pp. 440–441, Mar. 2015.
[33] B. Yang, M. Chen, and L. Li, "Design of a four-element WLAN/LTE/UWB MIMO antenna using half-slot structure," *AEU-Int. J. Electron. Commun.*, vol. 93, pp. 354–359, Sep. 2018.
[34] S. S. Jehangir and M. S. Sharawi, "A compact single-layer four-port orthogonally polarized Yagi-Like MIMO antenna system," *IEEE Trans. Antennas Propag.*, vol. 68, no. 8, pp. 6372–6377, Aug. 2020.
[35] S. Alkaraki and Y. Gao, "Mm-wave low-cost 3D printed MIMO antennas with beam switching capabilities for 5G communication systems," *IEEE Access*, vol. 8, pp. 32531–32541, Jan. 2020.
[36] W. Ali, S. Das, H. Medkour, and S. Lakrit, "Planar dual-band 27/39 GHz millimeter-wave MIMO antenna for 5G applications," *Microsyst. Technol.*, pp. 1–10, Jul. 2020, doi: 10.1007/s00542-020-04951-1.
[37] M. N. Hasan, S. Bashir, and S. Chu, "Dual band omnidirectional millimeter wave antenna for 5G communications," *J. Electromagn. Waves Appl.*, vol. 33, no. 12, pp. 1581–1590, Aug. 2019.
[38] N. Ashraf, O. M. Haraz, M. M. M. Ali, M. A. Ashraf, and S. A. S. Alshebili, "Optimized broadband and dual-band printed slot antennas for future millimeter wave mobile communication," *AEU-Int. J. Electron. Commun.*, vol. 70, no. 3, pp. 257–264, Mar. 2016.
[39] A. I. Sulyman, A. T. Nassar, M. K. Samimi, G. R. Maccartney, T. S. Rappaport, and A. Alsanie, "Radio propagation path loss models for 5G cellular networks in the 28 GHZ and 38 GHZ millimeter-wave bands," *IEEE Commun. Mag.*, vol. 52, no. 9, pp. 78–86, Sep. 2014.
[40] A. I. Najam, Y. Duroc, and S. Tedjini, "Multiple-input multiple-output antennas for ultra-wideband communications," *IntechOpen*, vol. 10, pp. 209–236, Oct. 2012.

ARPAN DESAI received the B.E. degree in electronics and communication engineering from Sardar Patel University, India, in 2006, the M.Sc. degree in wireless communication systems from Brunel University, London, U.K., in 2008, and the Ph.D. degree in transparent antennas from the Charotar University of Science and Technology, India, in January 2020. He worked as an Assistant Professor with the Department of Electronics and Communication Engineering, Charotar University of Science and Technology. He is currently working as a Postdoctoral Researcher with Ton Duc Thang University, Ho Chi Minh City, Vietnam. He has published more than 40 research articles, mostly in SCI/Scopus journals and international conferences. His current research interests include transparent antennas for MIMO applications, energy harvesting devices, transparent DRAs, and flexible wearable antennas.

CONG DANH BUI received the B.S. degree in electronics and telecommunications from the Ho Chi Minh University of Science and Technology, Vietnam, in 2018. He is currently pursuing the master's degree with the Faculty of Electrical and Electronics Engineering, Ton Duc Thang University, Ho Chi Minh City, Vietnam. His current research interests include circularly polarized antennas, metamaterial-based antennas, and reconfigurable antennas.

JAY PATEL (Graduate Student Member, IEEE) received the B.Tech. degree in electronics and communication from the Charotar University of Science and Technology (CHARUSAT), Changa, India. He is currently pursuing the M.Sc. degree in electrical and computer engineering with the New York Institute of Technology, New York, NY, USA. He is also working as a Graduate Assistant with the College of Engineering and Computer Science (CoECS), New York Institute of Technology. His current research interests include surface integrated waveguide (SIW) based antenna and cavity backed spiral antenna.

TRUSHIT UPADHYAYA (Senior Member, IEEE) received the B.E. degree from Gujarat University, in 2004, the M.E. degree from the Institute of Telecommunication Research, University of South Australia, Adelaide, in 2007, and the Ph.D. degree in satellite antennas from the Charotar University of Science and Technology (CHARUSAT), Changa, in 2014. He was a Visiting Scientist with the Physical Research Laboratory (PRL), Ahmedabad. He is currently working as a Professor and the Head of Department with the Department of Electronics and Communication Engineering, Faculty of Technology and Engineering, CHARUSAT. His research interests include antenna system design and applied electromagnetics. He has carried out research and consultancy projects for Australian defense agencies, Indian Space Research Organization (ISRO), Gujarat Council on Science and Technology (GUJCOST), and private organizations. He has published and presented several research articles in his area of research in India and abroad and he has delivered invited talk at various organizations across Gujarat.

GANGIL BYUN (Member, IEEE) received the B.S. and M.S. degrees in electronic and electrical engineering from Hongik University, Seoul, South Korea, in 2010 and 2012, respectively, and the Ph.D. degree in electronics and computer engineering from Hanyang University, Seoul, in 2015. After his graduation, he returned to Hongik University to work as a Research Professor and performed active research for two years. He joined the Faculty Member of the Ulsan National Institute of Science and Technology (UNIST) in February 2018, where he is currently an Assistant Professor of electrical engineering. His research interests include design and analysis of small antenna arrays for adaptive beamforming applications, such as direction of arrival estimation, interference mitigation, and radar. His current research interests include display-integrated antennas, optically-invisible antennas, and wireless backhaul antennas for 5G communications. He has actively contributed to the consideration of both antenna characteristics and signal processing perspectives for the improvement of overall beamforming performances.

TRUONG KHANG NGUYEN (Member, IEEE) received the B.S. degree in computational physics from the University of Science, Vietnam National University, Ho Chi Minh City, Vietnam, in 2006, and the M.S. and Ph.D. degrees in electrical and computer engineering from Ajou University, Suwon, South Korea, in 2013. From October 2013 to December 2014, he worked as a Postdoctoral Fellow with the Division of Energy Systems Research, Ajou University. He is currently an Assistant Director and the Head of the Division of Computational Physics, Institute for Computational Science, Ton Duc Thang University, Ho Chi Minh City. His current research interests include microwave antennas for wireless communication, terahertz antennas for compact and efficient sources, nanostructures and nanoantennas for optical applications, and computational micro/nano fluidics and heat transfer.